International Journal of Modern Physics D, Vol. 11, No. 2 (2002) 245–257

DYNAMICS OF EJECTION FROM GALAXIES AND THE VARIABLE MASS HYPOTHESIS

J. V. NARLIKAR and R. G. VISHWAKARMA
Inter-University Centre for Astronomy and Astrophysics, Post Bag 4, Ganeshkhind, Pune-411007, India

S. K. BANERJEE
Mody College of Engineering and Technology, Lakshmangarh, 332311, India

P. K. DAS
Indian Institute of Astrophysics, Koramangala, Bangalore 560034, India

H. C. ARP
Max Planck Institut fur Astrophysik, 85740 Garching, Germany

Received 29 May 2001
Communicated by K. Sato

Increasing numbers of active galaxies with significant alignments of quasars are being observed. It is the purpose of this paper to explore ejection dynamics of these quasars using the variable mass hypothesis (VMH) originally discussed by Narlikar and Das in 1980. According to the VMH quasars are ejected from parent galaxies initially with zero rest mass which grows through a Machian interaction. The intrinsic redshift of the quasar steadily decreases as its mass grows, but always remains in excess of the redshift of the galaxy. The ultimate aim of this hypothesis is to quantitatively relate the observed ordering of redshifts of ejected quasars, with separation from the galaxy, their intrinsic redshifts and the age of the evolutionary stage of the ejecta.

1. Introduction

Two decades ago, Narlikar and Das[15] had applied a modified version of the Hoyle–Narlikar theory of conformal gravity,[7] as developed by Narlikar[11] to work out the dynamical details of quasars ejected from galaxies. The Hoyle–Narlikar theory is based on the Machian idea that inertia of a particle of matter is determined through its long range scalar interaction with the rest of the matter in the universe. The modification proposed by Narlikar applies to newly created matter. To understand it let us first describe the spacetime of the universe by the Minkowski line element

$$ds_{\mathrm{M}}^2 = d\tau^2 - dr^2 - r^2(d\theta^2 + \sin^2\theta\, d\phi^2)\,. \tag{1}$$

A particle Q, created at time $\tau = \tau_Q > 0$, begins to interact with the rest of the matter in the universe after the moment of creation. Because the inertial interaction travels on the light cone, at any subsequent time τ, the particles within the sphere of radius $(\tau - \tau_Q)$ will contribute to inertia of the newly created particle. (We have taken the speed of light c equal to unity.) Consequently, the inertial mass of the particle is zero at creation and will grow as it ages.

It should be emphasized here that this state of zero rest mass is not like that of a photon, which *always* has zero rest mass. This is because the photon is not subject to the inertial interaction that ordinary matter is. Indeed, the original Hoyle–Narlikar theory of inertial interaction was patterned on the action at a distance electrodynamics of Wheeler and Feynman,[17] in which the photon does not exist as an independent particle as there is no electromagnetic field with its own independent degrees of freedom. Rather the electromagnetic effects are conveyed through the so-called *direct particle fields* which are entirely defined in terms of their source charged particles. As shown by Hoyle and Narlikar,[8,9] all well known effects of quantum electrodynamics can be explained in terms of this picture, *without recourse to a quantization of the electromagnetic field*, i.e. without admitting the existence of photons as independent particles. When electric charges interact, they do so nonlocally through direct particle fields which are essentially Green's functions having support on the light cones.

Therefore, in the above Machian theory, the inertia of a material particle (as opposed to that of a photon) grows after its creation, from an initial value zero, as it comes in contact with other particles through its inertial interaction. The field equations of this theory at a classical level have been discussed in detail elsewhere (see Ref. 11). Here we will discuss their applications to the dynamics of creation of quasars in galactic nuclei, and their ejection therefrom. The basic problem is posed as follows.

We will argue that most of the matter in the local universe was created at the same time, $\tau = 0$, and that the typical galaxy G, at epoch τ in this universe, assumed homogeneous and isotropic, would have a particle mass varying as τ^2. However, the typical particle mass in a quasar created and ejected from the galaxy at epoch τ_Q, would have a particle mass proportional to $(\tau - \tau_Q)^2$. Since the spectral wavelengths scale as reciprocal of the emitting particle mass, an observer receiving light from this galaxy at time τ_0, would find it redshifted by

$$z_{\mathrm{G}} = \frac{\tau_0^2}{\tau_{\mathrm{G}}^2} - 1\,, \tag{2}$$

where τ_{G} is the epoch when the light left the galaxy. Thus in this description galaxy redshifts arise in a static universe, the usual effect ascribed to the expansion of the universe being replaced here by the notion of variable mass. Narlikar and Arp[13] [see also, Ref. 14], had developed this "static universe model" and shown it to be consistent with cosmological observations. In this paper, however, a slightly

different notation was used and the t and τ coordinates were interchanged, i.e. the former was used in Eq. (1) above.

The Hoyle–Narlikar equations are fully written out below:

$$\frac{1}{2}m^2\left(R_{ik}-\frac{1}{2}g_{ik}R\right)=-3T_{ik}+m(\Box m g_{ik}-m_{;ik}) \\ +2\left(m_{,i}m_{,k}-\frac{1}{4}m^{,l}m_{,l}g_{ik}\right), \tag{3}$$

where the derivative terms arise in the field equations because of variability of the mass function m with coordinates. These equations are conformally invariant. That is, under a conformal transformation $ds \to \Omega \times ds$, the mass transforms as $m \to \Omega^{-1} \times m$. By a suitable choice of the conformal function Ω, one can make m a constant. Under such a transformation, for example, the static line element (1) gets changed to the Friedmann–Robertson–Walker line element describing an expanding universe.

Although the static universe picture is fully equivalent to the expanding universe paradigm for the overall population of such galaxies, differences between the two pictures arise for matter of subsequent origin (i.e. that created at epochs $\tau > 0$). For the quasar ejected by the above galaxy would have the redshift

$$z_Q = \frac{\tau_0^2}{(\tau_G - \tau_Q)^2} - 1\,. \tag{4}$$

Thus in general, any matter created subsequent to the universal creation epoch $\tau = 0$ will show an excess redshift with respect to matter created at the $\tau = 0$ epoch. In the above example, we shall write the excess component as the "intrinsic component", z_i as follows:

$$1 + z_Q = (1 + z_G)(1 + z_i)\,. \tag{5}$$

We will refer to the above redshift hypothesis as the "*Variable Mass Hypothesis* (*VMH*)." In actual observation we may find such a quasar–galaxy pair with discrepant redshifts, but with small enough separation to suggest that the former was ejected by the latter.

Returning to the Hoyle–Narlikar field Eqs. (3), we note the following result discussed in an earlier paper by two of us.[13] The mass terms oppose gravity in providing a static solution of the kind described in (1). In a collapsed massive object such as the nucleus of a galaxy, these repulsive forces arise whenever there is creation of new matter. Since these forces act against the gravitational binding of the nucleus, they can build up to a level that breaks up the nucleus and ejects a part of it. The part ejected consists of coherent objects of new matter because its mass is low and it moves rapidly under the repulsive forces. This mass, however, increases with time because of the Machian interaction with other particles in the universe. The typical ejected matter therefore starts with extremely high (literally infinite) redshift, as given by the formula (4). This high redshift declines with time,while

these coherent objects evolve and are seen as quasars with moderately large ($<\sim 5$) redshifts.

As has been argued by Narlikar and Arp,[14] the physics of these objects is controlled by conformally invariant equations. Because of this conformal invariance, the physics of a quasar made of new low mass particles, can be easily interpreted and understood as physics of a high redshift object with standard mass, by using the mass transformation discussed earlier. The only difference between the variable mass hypothesis and standard cosmology is that this hypothesis permits objects of different redshifts to be close neighbours, assuming that the higher redshift object (usually a quasar) has been ejected from the lower redshift one (e.g. a galactic nucleus).

It is worth stating here that the process may also be ejecting smaller objects of, say, stellar order. However, these will be much less luminous than quasars which contain many times more particles. Thus we expect to see only the biggest and brightest objects created in this process. Indeed, to understand ordinary stars one should invoke the usual scenario of condensation from gas clouds in galaxies. To explain stars the above creation and ejection process is neither necessary nor is it efficient. Rather, the process works well for understanding the highly energetic quasars and companion galaxies of significantly high redshifts found near galaxies of low redshifts.

It is generally argued that such discrepant cases are not real but arise from artefacts or chance projection effects. Considerable literature exists on this controversial issue [see e.g. a review by Narlikar[12] presenting both sides of the argument]. Here we sidestep the controversy, and assuming that the anomalous cases discussed here are genuine, pose the following question:

"Given the observed details of redshifts and angular separations, can we calculate the details of the ejection process?"

Narlikar and Das[15] had earlier shown how this can be done. However, the recent findings by Arp and others (for references see Ref. 1) include many new examples from X-ray astronomy, and it becomes pertinent to ask whether the Narlikar–Das picture proposed twenty years ago stands up to the recent data. In this paper we shall solve the dynamical equations of ejection for specific cases, as they will give us some idea of the physical conditions of ejection. We begin by summarizing the main results of Narlikar and Das[15] to be used here. For ready reference to that paper, referred to hereafter as Paper I, we will use the notation used therein, with a few minor alterations.

2. Dynamics of Ejection

2.1. *The spacetime line element*

We will consider the case of ejection in an almost radial direction outward from the nucleus (assumed spherical in this approximation) of a galaxy of mass M. Taking the radial coordinate as R, the time coordinate as T and the angular coordinates

as θ and ϕ, the line element of spacetime outside the mass can be approximated in the local region, by the standard Schwarzschild one:

$$ds^2 = \left(1 - \frac{2M}{R}\right) dT^2 - \left(1 - \frac{2M}{R}\right)^{-1} dR^2 - R^2(d\theta^2 + \sin^2\theta\, d\phi^2)\,. \tag{6}$$

Here we have set the gravitational constant $G = 1$. This line element will not be valid far away from the mass M, where we have to take into account the cosmological boundary conditions.

In this asymptotically far away region, the cosmological line element is given by (1), but which can be conformally transformed to the line element of the standard expanding universe (the Einstein de Sitter model). It is the latter frame to which (6) should be matched asymptotically. The advantage of choosing this standard line element is that in it the masses of particles in the galaxy are constant with time. Using the t coordinate, related to the τ coordinate of the static frame, by the relation $12t = \tau^3$, we get the cosmological line element as

$$ds^2 = dt^2 - \left(\frac{3t}{2}\right)^{4/3} [dr^2 + r^2(d\theta^2 + \sin^2\theta\, d\phi^2)]\,, \tag{7}$$

where the line elements (1) and (7) are related by the conformal transformation

$$ds^2 = \left[\frac{3t}{2}\right]^{4/3} \times ds^2_{\mathrm{M}}\,. \tag{8}$$

We have also taken the present value of Hubble's constant H_0 to be unity, so that the value of the present epoch in t coordinate is $2/3$. We will restore the c.g.s. units at a stage when observations are to be explicitly used.

The relationship of the (t, r) coordinates to the (T, R) system is defined by the following transformation:

$$R = r\left(\frac{3t}{2}\right)^{2/3}, \qquad T = \frac{2}{3}\left[\frac{1}{2}r^2 + \left(\frac{3t}{2}\right)^{2/3}\right]^{3/2}. \tag{9}$$

In terms of these coordinates the line element (6) becomes

$$ds^2 = e^{\nu} dT^2 - e^{\lambda} dR^2 - R^2(d\theta^2 + \sin^2\theta\, d\phi^2)\,. \tag{10}$$

As shown in Paper I, in the quasar–galaxy configurations, $T \approx t$ and $R \ll T$, and a good approximation for e^{ν} and e^{λ} is given by

$$\begin{aligned} e^{\nu} &\approx 1 + \frac{2}{9}\left(\frac{R}{T}\right)^2 + O\left(\frac{R}{T}\right)^4, \\ e^{\lambda} &\approx 1 + \frac{4}{9}\left(\frac{R}{T}\right)^2 + O\left(\frac{R}{T}\right)^4. \end{aligned} \tag{11}$$

How do we combine the asymptotic region with the local one? As discussed in Paper I, for the magnitudes of the parameters involved, a good approximation is given by:

$$\begin{aligned} e^{\nu} &\approx 1 - \frac{2M}{R} + \frac{2}{9}\left(\frac{R}{T}\right)^2 + \cdots , \\ e^{\lambda} &\approx 1 + \frac{2M}{R} + \frac{4}{9}\left(\frac{R}{T}\right)^2 + \cdots . \end{aligned} \tag{12}$$

In our calculations the time scales and distances involved for ejected material will be small enough compared to cosmological times and distances to justify the above approximation. We will next consider the equations of motion of a quasar ejected from the central mass.

2.2. *Equations of motion*

For a quasar with variable mass m, leaving the central mass and travelling radially outwards, the equation of motion is given by

$$\frac{d}{ds}\left(m\frac{dx^i}{ds}\right) + m\Gamma^i_{kl}\frac{dx^k}{ds}\frac{dx^l}{ds} = g^{ik}m_{,k}\,. \tag{13}$$

Here m depends on t only and through its dependence on T and R, on these coordinates. A little algebra worked out as in Paper I, leads to the following two equations:

$$\dot{R} = xe^{(\nu-\lambda)/2}\,, \tag{14}$$

$$\begin{aligned} &\dot{x} + (1-x^2)\left[\frac{M}{R^2} + \frac{d}{dt}(\ln m)\left\{x - \frac{2R}{3T}\left(1 - \frac{2M}{R}\right)\right\}\right] \\ &\quad + \frac{2R}{9T^2}\left[1 - x^2 - \frac{2R^2x(1-x^2)}{T(R-2M)}\right] = 0\,. \end{aligned} \tag{15}$$

Here overhead dot denotes differentiation with respect to $T \approx t$. The various terms on the left hand side denote the effects like those of the gravity of the central mass, the variability of the quasar mass and the expansion of the universe.

2.3. *A numerical solution*

The two equations above cannot be solved analytically, and so we adopt the numerical approach of Paper I. Assuming that the central mass has a finite radius, we set $R_1 = 1/10$ of that radius, say, and start the outward radial motion of the ejected quasar at this value of R. Generally ejection is along the line of least resistance, which is along the minor axis of the galaxy. One may wonder, why an object flying out with the speed of light should be hampered in any way by material en-route. The reason for this is as follows. The radial size of a particle goes as the reciprocal

of its mass (e.g. the Compton wavelength of a particle of mass m is $\hbar/mc$). Thus the characteristic cross section of a particle vis-a-vis its interaction with surrounding matter will go as m^{-2}. A young quasar made of such particles of low mass, will therefore encounter greater resistance from the surrounding gas and dust in a galaxy, than would an old quasar. The tendency for the ejected quasars will therefore be to prefer the line of least resistance, which naturally lies along the minor axis of an elliptical galaxy or perpendicular to the disc of a spiral galaxy.

Let $T = T_{\mathrm{Q}}$ denote the time of ejection, which is given in terms of the cosmological coordinate τ_{Q}, and hence t_{Q} mentioned earlier. The quasar starts out with an initial speed equal to that of light, but slows down as its mass grows. Even if there were no force of gravity from the parent galaxy, conservation of momentum would lead to a decrease of velocity. Not surprisingly, in the early stages of ejection the variable mass term $d(\ln m)/dt$ is the dominant one and retaining only this term, the equation of motion can be integrated analytically to give

$$\dot{R} \simeq \left(1 - \frac{2M}{R}\right) \left\{1 + A \left(\frac{T^{1/3} - T_{\mathrm{Q}}^{1/3}}{T^{1/3}}\right)^4\right\}^{-1/2}, \tag{16}$$

where A is a constant of integration. From this we see that the quasar was initially fired along a null trajectory, which is not surprising since it had zero rest mass at the time T_{Q} of ejection. However, its trajectory immediately becomes timelike since its mass starts growing for $T > T_{\mathrm{Q}}$. For this early phase of ejection write $T = T_{\mathrm{Q}} + \eta$, where η is small compared to T_{Q}. We then get the above solution in the form

$$\dot{R} \simeq \left[1 + \left(\frac{\eta}{\eta_0}\right)^4\right]^{-1/2}, \qquad \eta_0 = 3T_{\mathrm{Q}} A^{-1/4}. \tag{17}$$

The corresponding special relativistic time dilatation factor is therefore

$$\gamma \simeq \left(\frac{\eta_0}{\eta}\right)^2 \left[1 + \left(\frac{\eta}{\eta_0}\right)^4\right]^{1/2}. \tag{18}$$

The parameter η_0 characterizes the initial energy of ejection, indicating the time span over which the motion is relativistic. For example, we can take $\gamma = \sqrt{2}$ which happens at $\eta = \eta_0$ as the transition point from relativistic to nonrelativistic motion. The larger the value of η_0, the longer does the quasar travel relativistically. Let $R(\eta_0)$ denote the R-coordinate of the quasar at the end of the relativistic phase.

For later motion, i.e. starting with $T = T_{\mathrm{Q}} + \eta_0, R = R(\eta_0)$, we calculate R numerically from the full Eqs. (14) and (15). The specific examples will be discussed in the following section. Here we mention the general features of the expected solutions.

For a given η_0, we can continue the numerical integration till the epoch T_{G} when the light rays left the quasar and the galaxy, so as to arrive at the observer at the present epoch. Two alternatives are possible: (i) the value of R stops increasing

and begins to decrease, which means that the quasar is bound to the galaxy, and the radial orbit is in fact an approximation to a highly eccentric but closed orbit around the mass M; (ii) the quasar keeps moving outwards from the galaxy, i.e., there is no evidence till today's observations to say whether the quasar is bound to the galaxy.

In the first case we will call the quasar "Bound". If we increase the value of the ejection parameter η_0 continuously, the maximum coordinate distance $R_{\max}(\eta_0)$ reached by the quasar before turning back will increase, till we arrive at a limiting value of the ejection parameter for which the maximum distance is reached at the epoch $T_{\rm G}$. We will denote this value of the ejection parameter by $\eta_{\rm c}$. For an ejection parameter exceeding this value, we move on to the alternative (ii). Thus, in a limited sense this parameter plays the role somewhat like that of the escape velocity for a massive object.

In the first case, a small value of η_0 causes the path to turn around sooner. If we consider it an approximation to a highly eccentric orbit, then we will find that, as time passes, R oscillates with decreasing periods, between limits that shrink with time. This is because as the mass of the quasar grows with time, while its angular momentum remains conserved, its orbit will secularly shrink.

3. Applications to Quasars

We shall apply the above analysis to the following systems:

(i) The galaxy NGC 3516 with five quasars,[5]
(ii) The galaxy NGC 4258 with two quasars,[1]
(iii) The galaxy NGC 5985 with six quasars,[2]
(iv) The galaxy IC 4553 (Arp 220) with four companions.[3]

In all these cases, to translate the calculations into observable numbers, we need to estimate the mass M and the starting radial value R_1 from the observations of the galaxy. Such observations as are available to date, can give indicative values only, and the significance of the values chosen is no more than that. However, we will take one illustrative case, that of NGC 3516 of Table 1, in which we will increase the mass by a factor ~ 3 and likewise increase R_1 by a factor ~ 3, to see how the results get affected. We next compute the times $T_{\rm Q}$ when the quasars were created and ejected from the galaxy, and the time $T_{\rm G}$, when the light left the quasar/galaxy in order to reach us now. These epochs follow from the formulae given in earlier sections, in terms of the redshifts of the galaxy and the quasar (see Paper I):

$$T_{\rm Q} \approx \frac{2}{3}[(1+z_{\rm G})^{-1/2} - (1+z_{\rm Q})^{-1/2}]^3\,, \quad T_{\rm G} \approx \frac{2}{3}(1+z_{\rm G})^{-3/2}\,. \tag{19}$$

Next, from the observed angular separation $\theta_{\rm QG}$, we compute the projected linear separation of the quasar from the galaxy. For this purpose we use the galaxy redshift as the distance indicator of the system. Next we try numerical integration with the η_0 parameter. We change it progressively until we reach the critical value

η_c at which the quasar velocity just reaches the zero value for the first time at the epoch T_G. If at this stage the separation of the quasar is greater than the observed one, it means that the quasar is a bound one. We next compute the value of η_0 which gives the observed separation at T_G. This is the alternative (i) discussed in the last section. If the case belongs to alternative (ii), we conclude that there is no evidence that the quasar is bound to the galaxy.

Tables 1–4 give details for the four quasar–galaxy systems mentioned above. For measurement of distances we have used $H_0 = 50$ km·s^{-1}·Mpc^{-1}. In each table, the first column lists the quasars found in the vicinity of the concerned galaxy, the second column their redshifts and the third column their observed radial separations from the parent galaxy. The fourth column lists the critical values η_c of the ejection parameter, and the fifth column the values η_0 that produce the observed separations at the time of observation. [As a projection angle could be involved in relating the observed separation to the real one, we have taken it to be 45 degrees, which gives a mean deprojected value.] Column 6 shows the computed velocities of the ejected quasars at the time of observation. The last column tells us whether the quasar is bound (B: $\eta_0 < \eta_c$) or possibly unbound (U: $\eta_0 > \eta_c$).

Table 1. NGC 3516
Redshift(z_G) = 0.009, $M = 3 \times 10^{10} M_\odot$, $\theta_G = 1.8'$.

Object	Redshift (z_Q)	Radial Separation (kpc)	$\eta_c \times 10^6$	$\eta_0 \times 10^6$	Velocity at T_G +ve outward −ve inward (km/s)	Status: Bound/ Unbound
Q1107+7232	2.1	94.84	6.84	5.95	−32.3	B
Q1105+7238	1.4	162.15	5.08	4.66	−16.1	B
Q1105+7242	0.93	240.17	3.45	3.35	−5.2	B
Q1106+7244	0.69	226.62	2.45	2.36	−7.8	B
Q1108+7226	0.33	245.42	0.80	0.77	−6.8	B

Table 2. NGC 4258
Redshift(z_G) = 0.002, $M = 7.5 \times 10^{10} M_\odot$, $\theta_G = 4.5'$.

Object	Redshift (z_Q)	Radial Separation (kpc)	$\eta_c \times 10^6$	$\eta_0 \times 10^6$	Velocity at T_G +ve outward −ve inward (km/s)	Status: Bound/ Unbound
X-ray	0.40	42.28	1.79	1.64	−111.8	B
X-ray	0.65	47.68	3.38	3.05	−102.9	B

Table 3. NGC 5985(Sey1)
Redshift($z_{\rm G}$) = 0.008, $M = 7.5 \times 10^{10} M_{\odot}$, $\theta_{\rm G} = 1.25'$.

Object	Redshift ($z_{\rm Q}$)	Radial Separation (kpc)	$\eta_{\rm c} \times 10^6$	$\eta_0 \times 10^6$	Velocity at $T_{\rm G}$ +ve outward −ve inward (km/s)	Status: Bound/ Unbound
HS1543+5921	0.807	718.05	4.21	5.18	27.7	U
RXJ15509+5856	0.348	1759.11	1.39	2.90	86.7	U
SBS1537+595	2.125	233.51	9.55	8.77	−17.3	B
SBS1535+596	1.968	490.37	9.10	10.20	13.1	U
SBS1533+588	1.895	1056.63	8.88	16.66	50.3	U
SBS1532+598	0.69	937.93	3.53	4.98	41.6	U

Table 4. Arp 220(IC 4553)
Redshift($z_{\rm G}$) = 0.018, $M = 10^{13} M_{\odot}$, $\theta_{\rm G} = 0.75'$.

Object	Redshift ($z_{\rm Q}$)	Radial Separation (kpc)	$\eta_{\rm c} \times 10^6$	$\eta_0 \times 10^6$	Velocity at $T_{\rm G}$ +ve outward −ve inward (km/s)	Status: Bound/ Unbound
Arp No. 2(RSO)	1.26	301.44	32.98	29.08	−448.7	B
Arp No. 9(BSO)	1.25	344.5	32.75	28.93	−408.9	B
20.N	0.23	1283.27	3.67	3.52	−110.7	B
20.3S	0.46	1856.0	10.75	10.59	−22.7	B

To see how robust these conclusions are vis-a-vis the parameters R_1 and M of the ejecting galaxy, we considered the cases where (a) the mass of the galaxy was increased by a factor three, (b) the radius R_1 was increased by a factor three, and (c) both mass and radius were increased by factor three. As expected, the values of $\eta_{\rm c}$ and η_0 are different for these different cases. When the mass is increased by a factor 3, the value of $\eta_{\rm c}$ increases approximately by a factor 1.5, and a similar change occurs in the value of η_0, while the corresponding increase in the value of R_1 does not produce a significant increase in $\eta_{\rm c}$ or η_0. However, the final conclusion as to whether the quasar is bound or not, remains the same. In any case, we should look at the tabulated values as indicative only with the same degree of accuracy as ascribed to standard Newtonian galactic dynamics.

Figures 1 and 2 illustrate the findings for the case (i). Table 1 shows that all five quasars in this case are bound, that is, their observed angular separations are less than the maximum separation for a bound quasar. In Fig. 1 we show that the maximum separation decreases as the quasar redshift increases. The five observed

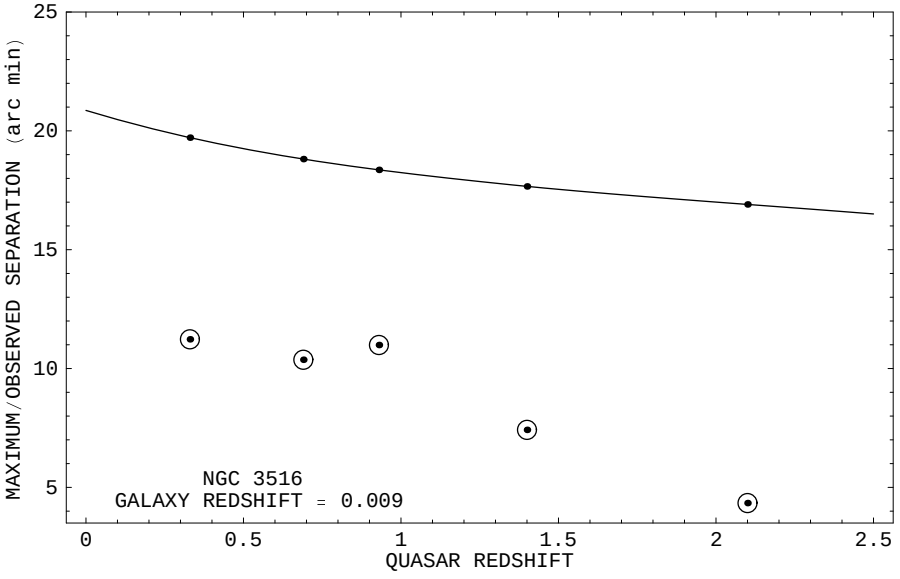

Fig. 1. This shows that the maximum separation between the quasar and galaxy decreases as the quasar redshift increases. The observed points are shown by open circles.

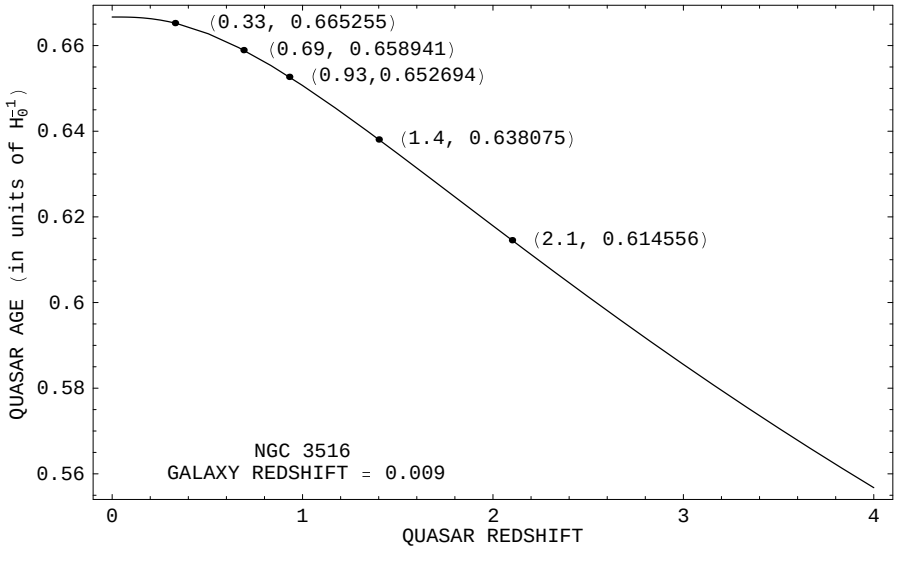

Fig. 2. Quasar age against its redshift: the larger redshift quasars are younger.

points lie below the continuous curve denoting the maximum separation for the specified quasar redshift. Figure 2 shows the quasar age against its redshift; as predicted theoretically, the larger redshift quasars are younger. Similar figures can be drawn for the other three ejection systems.

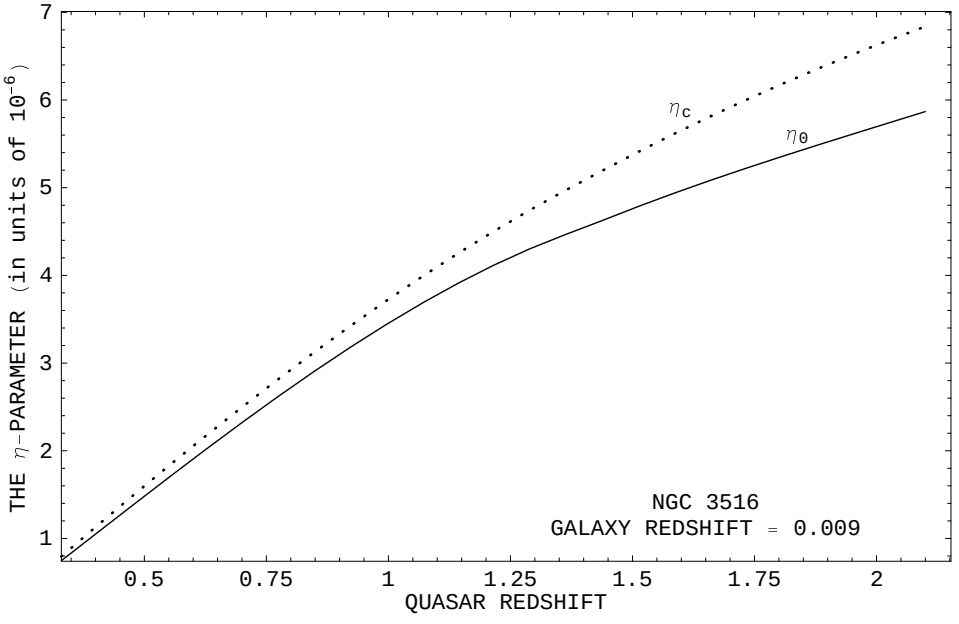

Fig. 3. The escape velocities of the quasars diminish as their intrinsic redshifts get smaller. The above figure uses the parameter η_0, which indicates the time scale over which the ejected motion is relativistic. Thus the larger the value of this parameter, the faster is the outward motion of the ejecta, with η_c corresponding to the escape speed. The dotted line shows the value η_c while the continuous line shows the value η_0 for actual observations.

The velocities of the quasars given in the tables are expressed in kilometres per second, and are of the order of 10–400 km/s. This tells us that in this picture there is a very modest Doppler component of spectral shift in the quasar. Figure 3 shows the escape velocities of quasars against their intrinsic redshift as estimated by the parameter η_0. Note that for bound quasars the value of η_0 is less than the escape value η_c.

4. Conclusion

It is interesting to note that a consistent picture emerges from these calculations in which a typical quasar starts its life as a young lump of matter ejected from the parent galaxy with the speed of light and zero rest mass, which starts growing with age. As the redshift decreases with increasing mass, the quasar passes through a continuous sequence of decreasing redshifts. Whether it will altogether escape from the gravitational attraction of the galaxy will depend on the energy of initial ejection, measured here in terms of the parameter η_0. It is possible that some of the quasars seen in isolation are the "escaped" quasars. On the other hand the bound quasars will move in steadily shrinking orbits around the parent galaxy. Our calculation gives a method of deciding which quasars are bound.

This work is, however, entirely based on classical mechanics as modified by the Machian theory of gravity. It leaves unanswered why there should be quantized redshifts, as claimed from time to time (Refs. 4 and 6 for galaxies; and Refs. 10 and 16 for QSOs). The present formalism needs to have a quantum version to understand redshift periodicities. In terms of the VMH, this means mass quantization, which can control the onset of ejection. Assuming that the creation mechanism produces a local scalar field of negative energy and stresses, one can argue that the nucleus of the parent galaxy becomes unstable whenever the created mass attains one of a discrete set of values and ejects the same. Work is in progress, quantifying this idea and using it to understand the periodicity found in the redshifts of ejected quasars.

References

1. H. C. Arp, *Seeing Red* (Apeiron, Montreal, 1998).
2. H. C. Arp, *Astro* **341**, L5 (1999).
3. H. C. Arp, E. M. Burbidge and Y. Chu, 2001 (submitted).
4. T. J. Broadhurst, R. S. Ellis, D. C. Koo and A. S. Szalay, *Nature* **34**, 726 (1990).
5. Y. Chu, J. Wei, J. Hu, X. Zhu and H. C. Arp, *Astrophys. J.* **500**, 596 (1998).
6. J. Einasto, in *Cosmological Parameters and the Evolution of the Universe*, Proc. IAU Symp. 183, ed. K. Sato (Kluwer, Dordrecht, 1999), p. 169.
7. F. Hoyle and J. V. Narlikar, *Proc. Roy. Soc.* **A294**, 138 (1966).
8. F. Hoyle and J. V. Narlikar, *Ann. Phys.* (*N.Y.*) **A54**, 207 (1969).
9. F. Hoyle and J. V. Narlikar, *Ann. Phys.* (*N.Y.*) **A62**, 44 (1971).
10. K. G. Karlsson, *Astrophys.* **58**, 237 (1977).
11. J. V. Narlikar, *Ann. Phys.* (*N.Y.*) **107**, 325 (1977).
12. J. V. Narlikar, *Sp. Sc. Rev.* **50**, 523 (1989).
13. J. V. Narlikar and H. C. Arp, *Astrophys. J.* **405**, 51 (1993).
14. J. V. Narlikar and H. C. Arp, *Astrophys. J.* **482**, L119 (1997).
15. J. V. Narlikar and P. K. Das, *Astrophys. J.* **240**, 401 (1980).
16. W. Tifft, *Astrophys. J.* **268**, 56 (1983).
17. J. A. Wheeler and R. P. Feynman, *Rev. Mod. Phys.* **17**, 157 (1945).